Eur. Phys. J. A (2026) 62:70
https://doi.org/10.1140/epja/s10050-026-01806-7

THE EUROPEAN PHYSICAL JOURNAL A

Regular Article - Experimental Physics

Lifetimes of negative parity states in ^{162}Dy

A. Aprahamian[1,a], S. R. Lesher[2,3], C. Casarella[1], K. Lee[1], B. P. Crider[4], M. Lowe[3], M. M. Meier[3], E. E. Peters[5], F. M. Prados-Estévez[6], T. J. Ross[6], S. W. Yates[5,6]

[1] Department of Physics and Astronomy, University of Notre Dame, Notre Dame, IN 46556, USA
[2] Department of Physics, North Carolina A&T State University, Greensboro, NC 27411, USA
[3] Department of Physics, University of Wisconsin–La Crosse, La Crosse, WI 54601, USA
[4] Department of Physics and Astronomy, Mississippi State University, Starkville, MS 39762, USA
[5] Department of Chemistry, University of Kentucky, Lexington, KY 40506, USA
[6] Department of Physics and Astronomy, University of Kentucky, Lexington, KY 40506, USA

Received: 16 October 2025 / Accepted: 30 January 2026

Communicated by Silvia Leoni

Abstract Lifetimes of excited states in ^{162}Dy were measured using the (n,n'γ) reaction with the Doppler-Shift Attenuation Method (DSAM) at the University of Kentucky's Accelerator Laboratory. A total of eighteen level lifetimes were obtained, including eleven negative-parity states, seven of which are new. These measurements significantly expand the experimental database of transition probabilities for negative-parity bands in the well-deformed rare earth region of nuclei. The extracted B($E1$) and B($E2$) values reveal enhanced interband E1 (10^{-3} or 10^{-4}) W.u. and E2 strengths (several W.u.) between negative- and positive parity bands, particularly for the $K^\pi = 2^-_{1,2}$ bands decaying to the the $K^\pi = 2^+_\gamma$ band, consistent with signatures of octupole-quadrupole coupling. In contrast, the $K^\pi = 0^-_1$ and $K^\pi = 1^-_3$ bands, which exhibit strong E1 transitions to the ground state band, are indicative of octupole-vibrational excitations built on the deformed ground state. Comparison of transition rates with Alaga rules supports this interpretation and distinguishes collective excitations from likely quasi-particle states. These new results establish ^{162}Dy as the most extensively characterized rare-earth nucleus for negative parity lifetimes and provide critical experimental benchmarks for theoretical models.

1 Introduction

Nuclear structure is focused on building a coherent framework for describing the properties of nuclei. There have been significant advances in studying and characterizing properties of nuclei; however, challenges remain. One of those challenges revolves around the determination of the viability of the nucleus to sustain single or multiple quanta of vibrational oscillations superimposed on an equilibrium deformed shape of the nucleus. Typically, enhanced transition probabilities between excited bands and the ground state bands, indicate common components in the wave functions of the excited states with the ground state.

In phenomenological or geometric models, the lowest vibrational shape affecting excitations are ($\lambda = 2$) quadrupole or ($\lambda = 3$) octupole modes with predictions for the behavior in excitation energy ratios, and transition probabilities connecting them to the ground state band for single or multiple phonons. Extensive sets of lifetime measurements have been presented [1–3] for the low-lying positive parity excitations in ^{162}Dy, but far fewer level lifetimes exist for the negative parity states. A recent review addresses vibrational aspects extracted from lifetime and transfer reaction measurements [1] for the positive parity levels in comparison with several models. However, much less information has been available for the lifetimes of the negative parity states and the discussion of octupole (3^-) vibrational oscillations. Octupole oscillations ($\lambda = 3$) of a spherical nucleus or octupole-deformed nuclei have been identified in the actinides [4–6] and in the spherical/transitional nuclei (and in extremely neutron-rich ^{144}Ba) [7,8] by the observation of strong E3 transitions to the ground state. A recent study even reported on the identification of quadrupole $\times$ octupole states in the ^{208}Pb nucleus at 3.6 MeV [9]. In well-deformed nuclei, octupole vibrational modes are less well understood since the correlation of octupole and quadrupole oscillations are difficult to address microscopically, geometrically, or algebraically. An octupole phonon or oscillation with $\lambda = 3$ is expected to split into $K^\pi = 0^-, 1^-, 2^-$, and 3^-

[a] e-mail: aapraham@nd.edu (corresponding author)

Published online: 03 April 2026

excitations in the low lying spectra of deformed nuclei. The splitting and/or fragmentation of the octupole modes present distinct challenges. Complexities arise from the deformation of the ground state and the superposition of octupole and quadrupole oscillations. K-forbiddenness plays a role for the quartet of negative parity bands and the experimentally measured hindrances of transition probabilities or B($E1$) values for the ΔK>1 [8] bands in individual nuclei, but the full systematic evolution of any octupole strength across the range of fragmented negative parity states is yet to be established. Mean field and beyond calculations have shown soft octupole deformations near closed shells in the rare earth region that decrease with increasing quadrupole deformations [10]. Calculations [4,11–13] of collective Hamiltonians for the rotation-vibration motion of nuclei include interplays of quadrupole, β_2, and octupole, β_3, degrees of freedom in the rare-earth region for deformed nuclei such as ^{154,158}Gd and ^{156}Dy with enhanced $E1$ transitions between positive and negative parity states. The coupling of octupole and quadrupole vibrations have been reported in $K^\pi = 2^- \rightarrow K^\pi = 2^+_\gamma$ transitions (in the form of a $2^+ \otimes 3^-$ phonon coupling) and $J^\pi = 1^-$ states are interpreted as two-phonon excitations due to the coupling of octupole ($J^\pi = 3^-, K^\pi = 1^-$) and quadrupole γ-vibrations ($J^\pi = 2^+$, $K^\pi = 2^+$) in this nucleus [14] and several nearby cases [15,16], which mirror and expand upon the feasibility of multi-phonon states in deformed nuclei [17,18]. B($E3$) values however are generally lacking, as well as extensive sets of lifetime measurements of negative parity levels. The recognition of enhanced E1 transitions is fairly new and distinctly contrasted with the historical notion of octupole collectivity built on the ground state. Comparisons with data for this complex situation are limited. Although extensive studies have been undertaken on the low-lying structure of ^{162}Dy [2,3], there were only a handful of lifetime measurements of negative parity levels to ascertain the nature of the observed bands and the role of $E1$ transitions connecting the negative and positive parity states.

In this work, we report on the measurements of a large number of negative parity level lifetimes in ^{162}Dy using the $(n, n'\gamma)$ reaction and the Doppler-shift attenuation method at the University of Kentucky. The newly measured level lifetimes include eighteen in total. These include eleven lifetimes (7 new) for negative parity states and seven for levels of unknown parity.

2 Experiment

Levels in ^{162}Dy were excited using quasi-monoenergetic neutrons from a primary ^{3}H(p, n) reaction at the University of Kentucky Accelerator Laboratory (UKAL). Measurements included a γ-ray excitation function and angular distributions measured with the ^{162}Dy$(n, n'\gamma)$ reaction using a 96.17% enriched scattering sample of ^{162}Dy oxide powder. The 24.0 g scatter sample was contained in a thin-walled polyethylene cylinder 7.62 cm high and 3.81 cm in diameter. The emitted γ rays were detected with a 50% relative efficiency HPGe detector with time-of-flight gating for background suppression and a BGO shield for active Compton suppression [19].

The excitation function for this reaction was performed in 75 keV steps from $E_n = 1.4 - 3.1$ MeV with the detector placed at 90° with respect to the beam axis and used to confirm the established level scheme by checking the threshold of γ rays which have already been placed. These excitation functions provide γ-ray yields as a function of neutron energy. Angular distribution measurements were performed at incident neutron energies of 1.6, 2.2, and 3.1 MeV over an angular range of 40° to 150°. These neutron energies were chosen to reduce feeding to the levels of interest to promote accurate lifetime measurements. The angular distributions of the γ-ray intensities, W(θ), were fitted with even-order Legendre polynomials:

$$W(\theta) \approx a_0[1 + a_2P_2(\cos\theta_{lab}) + a_4P_4(\cos\theta_{lab})] \quad (1)$$

where the parameters a_2 and a_4 depend on the multipolarities and mixing amplitudes of the transitions. Multipolarity information (namely multipole mixing ratios, δ) for mixed-multipolarity transitions can be extracted from angular distribution coefficients using a statistical model code calculation [20]. The angular distributions also yield lifetimes of excited states shorter than about 1 ps [21] as determined by the Doppler shift attenuation method (DSAM), a technique that exploits the fact that any emitted radiation from a recoiling nucleus will be energy shifted with respect to the laboratory angle of observation. The γ rays have energies with angular dependence:

$$E_\gamma(\theta) = E^o_\gamma[1 + \beta F(\tau)\cos(\theta)] \quad (2)$$

The de-exciting γ rays will be Doppler shifted linearly as a function of $\cos(\theta)$, the unshifted γ-ray energy E^o_γ, the recoil velocity of the decaying nucleus β, and a lifetime attenuation factor F(τ), which depends on the nuclear stopping power [21]. A detailed analysis of the uncertainties associated with the nuclear stopping power is discussed in Ref. [21]. By examining the energy of a γ ray as a function of angle, the F(τ) value can be determined using the Winterbon formalism [22], and the lifetime of the state, τ, can be extracted [23]. Examples of γ rays and associated lifetimes are shown in Fig. 1. Lifetimes determined using γ rays arising from the same level must match within experimental uncertainties, providing additional consistency tests of placement and aiding in the assignment of γ rays to specific levels.

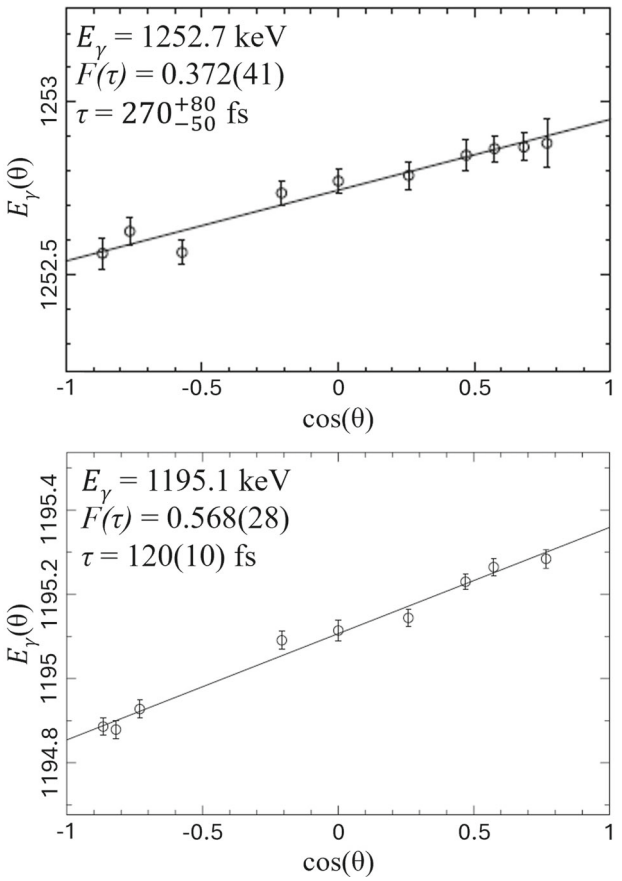

Fig. 1 Examples of Doppler energy shifts for two γ rays observed in the ^{162}Dy $(n, n'\gamma)$ reaction. The E_γ = 1252.7 keV shows a slight shift with a long lifetime while the E_γ=1195.1 keV shows a shorter lifetime

3 Results

We report on eleven negative and seven levels of unknown parity in ^{162}Dy. Fourteen of the levels are new (7 negative) and measured for the first time. Previously reported literature values are given in ENSDF [24]. Table 1 reports the levels with observed lifetime values from our work or those discussed in this paper. The reported information includes the γ rays observed, F(τ) values and associated level lifetimes in femtoseconds, measured relative intensities, and γ-ray energies in keV. Multipole mixing ratios (δ) are included when available. In some cases, our experiment would not allow differentiation of a previously observed γ ray from a background line. However, transitions and their intensities reported by ENSDF [24] were included when calculating the transition probabilities of all levels of interest with known lifetimes as reported in a separate table (Table 2). We have deliberately kept the transitions and lifetimes measured from our experiment and those reported by ENSDF separated in these two tables. In some cases, these include transitions that were too weak to be observed by our experiment, or they are strong transitions that lie on a complicated background set of lines (for example, the 543.1 keV line depopulating from the 1691.4 keV level), but they were seen in previous experiments and included in the evaluated data. All transition probabilities were calculated using TROPIC [25].

3.1 Negative parity bands

Direct measurements of $E3$ transitions are difficult since the γ-ray intensities are small. Measurements of $E1$ transition probabilities were always significantly lower than the theoretical Weisskopf estimates. B($E1$) transition probabilities can range from 10^{-10} to 1 W.u. Some decades ago, the $E1$ transitions were typically discussed in the context of giant resonances or reflection-asymmetric shapes and they were well established in the actinides. Butler and Nazarewicz [26] and many others afterwards, had suggested that enhanced B($E1$) values may in fact be related to the coupling of low-lying octupole one-phonon states to the quadrupole deformed states rather than the presence of reflection asymmetries. The assignments of B($E1$) values in the **milli-Weisskopf** range from negative parity states became accepted as **enhanced** and a signature of single octupole phonon excitations couplings to quadrupole deformed states. It had been also shown [27] that ΔK values also have a role in the enhancement or retardation of B($E1$) values. B($E1$) values connecting states with $\Delta K = 0$ are the most enhanced and decrease in several orders of magnitude as ΔK increases. The discussion is ongoing regarding the use of enhanced $E1$ transitions as signatures of octupole-quadruple correlations. Measurement of large B($E1$)s are not considered the "smoking gun" of octupole deformation, but are still indicative and critical in the determination of similar wave function components among strongly connected states or any single and/or double-phonon octupole characteristics in deformed nuclei [28].

Efforts have been ongoing to expand the lifetime information for negative parity states in the Dy isotopic chain. As of the most recent ENSDF evaluations, there are currently 4 lifetimes listed for ^{160}Dy [29] and 9 for ^{162}Dy [24]. For ^{164}Dy, level widths have been measured through photon-scattering experiments for 6 1^- states from 1.6 MeV to 4 MeV [30,31]. A recent photon-scattering study measured level widths for 32 additional 1^- states from 4 to 5 MeV [32]. In this work, we measured 11 lifetimes of negative parity states where 7 are measured for the first time. The lifetimes and the resulting transition probabilities represent an extensive set of $E1$ transitions connecting the positive and negative parity states in ^{162}Dy providing the foundation for identifying major wave function components and the possibility of distinguishing between quasi-particle excitations and collective states. All observed transitions from negative parity bands are shown in Figs. 3 and 4. An octupole vibrational excitation ($\lambda = 3$) is expected to fragment into a quartet of states with $K^\pi = 0^-$,

Table 1 Level energies (keV), γ-ray energies (keV), intensities, level F(τ) values, mean lifetimes (fs), and multipole mixing ratios, δ, observed in the current ^{162}Dy$(n, n'\gamma)$ experiment. The literature lifetimes, $\tau_{\rm lit}$, are from Ref. [24] unless otherwise noted. The ground-state band members are noted using "g" and γ rays which cannot be separated from multiple groupings are considered multiplets and noted. The quoted uncertainties on the lifetimes are only statistical

E_{lev} (keV)	E_γ (keV)	K_i^π, J_i^π	K_f^π, J_f^π	I_γ (rel)	F(τ)	τ (fs)	$\tau_{\rm lit}$ (fs) Ref. [24]	δ	Notes
1148.27(11)	260.16(21)	$2_1^-, 2^-$	$2^+, 2_\gamma^+$	100	–	–	$300(60) \times 10^3$		
1209.98(8)	247.25(21)	$2_1^-, 3^-$	$2^+, 3_\gamma^+$	10(1)	0.052(30)	3100^{+3700}_{-1200}	–		
	322.01(21)		$2^+, 2_\gamma^+$	15(1)					
	944.43(9)		$0^+, 4_g^+$	56(1)					
	1129.41(9)		$0^+, 2_g^+$	100(2)					
1275.73(9)	1195.11(9)	$0_1^-, 1^-$	$0^+, 2_g^+$	100(2)	0.568(28)	120(10)	29(6)		
	1275.82		$0^+, 0_g^+$	<65					1
1297.02(16)	236.09(21)	$2_1^-, 4^-$	$2^+, 4_\gamma^+$	18(1)	0.103(49)	1400^{+1500}_{-350}	–		
	334.15(21)		$2^+, 3_\gamma^+$	100(2)					
1357.86(11)	1092.27(9)	$0_1^-, 3^-$	$0^+, 4_g^+$	75(2)	0.612(43)	100(20)	< 210		2
	1277.33		$0^+, 2_g^+$	<100					1
1390.53(12)	1124.94(9)	$2_1^-, 5^-$	$0^+, 4_g^+$	100	0.090(82)	>920	–		
1485.71(10)	937.23(8)	$5^-, 5^-$	$0^+, 6_g^+$	35(2)	–	–	< 2910		3
	1220.16(8)		$0^+, 4_g^+$	100(3)					
1518.39(10)	970.01(9)	$0_1^-, 5^-$	$0^+, 6_g^+$	42(1)	0.372(41)	270^{+80}_{-50}	< 190		
	1252.74(9)		$0^+, 4_g^+$	100(2)					
1570.76(16)	212.89(20)	$3^-, 3^-$	$0_1^-, 3^-$	59(2)	–	–	–		
	295.23(20)		$0_1^-, 1^-$	100(2)					
1637.19(11)	427.62(50)	$1_1^-, 1^-$	$2_1^-, 3^-$	<16	–	–	–		1
	489.05(6)		$2_1^-, 2^-$	>11.1					
	1556.53(6)		$0^+, 2_g^+$	>72.5					
1669.13(24)	311.27(21)	$3_1^-, 4^-$	$0_1^-, 3^-$	100	0.289(116)	440^{+450}_{-210}	–		
1691.38(12)	415.57	$1_1^-, 2^-$	$0_1^-, 1^-$	<93	–	–	–		4 5
	728.50(9)		$2^+, 3_\gamma^+$	100(2)					
1739.01(9)	529.06(9)	$1_1^-, 3^-$	$2_1^-, 3^-$	100(2)	0.107(98)	>740	–	1.4(2)	
	590.74(9)		$2_1^-, 2^-$	37(2)				$1.2^{+0.5}_{-0.3}$	
	678.12(9)		$2^+, 4_\gamma^+$	63(2)					
	1473.36(9)		$0^+, 4_g^+$	66(1)					
1862.96(22)	327.13(20)	$4^-, 4^-$	$4_1^+, 4^+$	100	–	–	1580 – 2860		
1863.82(9)	900.91(9)	$2_2^-, 2^-$	$2^+, 3_\gamma^+$	34(1)	0.297(35)	420^{+120}_{-80}	–		
	975.65(9)		$2^+, 2_\gamma^+$	100(2)					
1910.46(9)	947.51(10)	$2_2^-, 3^-$	$2^+, 3_\gamma^+$	100(2)	0.250(63)	550^{+260}_{-180}	250 – 300		
	1022.32(9)		$2^+, 2_\gamma^+$	81(2)					
1973.05(10)	912.09(10)	$2_2^-, 4^-$	$2^+.4_\gamma^+$	33(2)	0.205(53)	780^{+280}_{-210}	–		
	1010.19(9)		$2^+, 3_\gamma^+$	100(2)	–				
2148.47(50)	2067.86(50)	(2)	$0^+, 2_g^+$	100	0.048(26)	3200^{+3500}_{-1200}	–		
2313.81(50)	2233.20(50)		$0^+, 2_g^+$	100	0.133(48)	1200^{+620}_{-290}	–		
2339.31(73)	2339.29(73)		$0^+, 0_g^+$	100	0.285(67)	480^{+230}_{-160}	–		
2386.54(50)	2305.93(50)		$0^+, 2_g^+$	100	0.217(53)	710^{+260}_{-190}	–		

Table 1 continued

E_{lev} (keV)	E_γ (keV)	K_i^π, J_i^π	K_f^π, J_f^π	I_γ (rel)	$F(\tau)$	τ (fs)	τ_{lit} (fs) Ref. [24]	δ	Notes
2488.05(77)	2407.44(77)		$0^+, 2_g^+$	100	0.270(52)	520^{+190}_{-140}	–		
2505.78(49)	2240.40(90)	(2^+)	$0^+, 4_g^+$	100(3)	0.500(32)	160(20)	–		6
	2505.66(59)		$0^+, 0_g^+$	98(4)					
2509.49(68)	2428.88(68)		$0^+, 2_g^+$	100	0.361(50)	290^{+100}_{-60}	–		

[1] This γ ray is embedded in a multiplet in the $(n, n'\gamma)$ reaction
[2] The intensity of this γ ray was scaled with respect to the intensity of the multiplet
[3] Ref. [24] lists $T_{1/2}$=1.92(11) ns, obtained from a β-decay study, as the recommended value for the lifetime of this level. It is possible that the extracted lifetime from the β-decay might have depopulated a different level or involved two γ rays that could not be resolved. We have adopted the value reported by Ref. [3], which was measured using the high precision GRID technique
[4] Ref. [24] lists that the 543.11 keV γ ray from this level has the strongest intensity. However, it was mixed with background lines on top of a neutron bump in our work. Therefore, we have decided to omit this γ ray from this table
[5] This γ ray is mixed with a background line in this work. The intensity of this γ ray was scaled with respect to the the 728.5 keV γ ray
[6] The spin and parity of this level could not be confirmed directly. However, the observed depopulating transitions to a 4^+ and a 0^+ state, along with the measured lifetime suggest that this level is likely a 2^+

Table 2 Transition probabilities calculated for bands of interest in ^{162}Dy. All transition probabilities were calculated using TROPIC [25]. The ground-state band members are noted using "g." Level energies (keV), γ-ray energies (keV), intensities, level lifetimes (fs), $M1/E2$ mixing ratios (δ), and relative intensities are from this $(n, n'\gamma)$ work and reported in Table 1 unless noted. If γ rays from previous measurements are added to the level, the relative intensities are adopted from that reference and normalized with the intensities of the observed transitions. Conversion coefficients (α_T) and assigned multipolarities are from Ref. [24]. For mixed transitions ($M1/E2$) without a known mixing ratio (δ), the B($E2$) value is reported assuming 100%E2. The B($E2$)s are reported in W.u. where 1 W.u. = 5.2461×10^{-3} e^2b^2. The B($E1$)s are reported in W.u. where 1 W.u. = 1.9155×10^{-2} e^2b. When our lifetime measurement provided a limit, we adopted the literature lifetime from Ref. [24] and denoted with a †

E_i (keV)	J_i^π	E_γ (keV)	K_f	J_f^π	E_f (keV)	I_γ (rel.)	α_T	τ (fs)	$\pi\ell$	B($E1$) or B($E2$)	Notes
$K^\pi = 2_1^-$											
1148.27	2^-	185.29	2	3_γ^+	963	20.0(8)	0.0595	$300(60) \times 10^{3\dagger}$	$E1$	$2.8^{+0.9}_{-0.6} \times 10^{-5}$	1
		260.16	2	2_γ^+	888	100(2)	0.0246		$E1$	$5.0^{+1.5}_{-1.0} \times 10^{-5}$	
		1067.55	0	2_g^+	81	0.70(2)	0.00111		$E1$	$5.0^{+1.6}_{-1.1} \times 10^{-9}$	1
1209.98	3^-	149.10	2	4_γ^+	1061	4.4(1)	0.1059	3100^{+3700}_{-1200}	$E1$	$7.5^{+5.4}_{-4.3} \times 10^{-4}$	1
		247.25	2	3_γ^+	963	10(1)	0.0281		$E1$	$3.8^{+3.2}_{-2.3} \times 10^{-4}$	
		322.01	2	2_γ^+	888	15(1)	0.01444		$E1$	$2.6^{+2.0}_{-1.5} \times 10^{-4}$	
		944.43	0	4_g^+	266	56(1)	0.00153(18)		$E1$	$3.8^{+2.7}_{-2.1} \times 10^{-5}$	
		1129.41	0	2_g^+	81	100(2)	0.00102(7)		$E1$	$3.9^{+2.8}_{-2.2} \times 10^{-5}$	
1297.02	4^-	86.92	2_1	3^-	1210	0.42(3)	4.1(6)	1400^{+1500}_{-350}	$M1/E2$	(See [a])	1
		114.24	2	5_γ^+	1183	5.9(4)	0.216		$E1$	$7.0^{+3.3}_{-4.0} \times 10^{-3}$	1
		236.09	2	4_γ^+	1061	18(1)	0.0316		$E1$	$2.4^{+1.1}_{-1.4} \times 10^{-3}$	
		334.15	2	3_γ^+	963	100(2)	0.01319		$E1$	$4.8^{+1.9}_{-2.6} \times 10^{-3}$	
		1031.36	0	4_g^+	266	2.8(1)	–		$E1$	$4.5^{+1.9}_{-2.5} \times 10^{-6}$	1
1390.53	5^-	180.41	2_1	3^-	1210	0.14	0.334(5)	>920	$E2$	<90	1
		329.52	2	4_γ^+	1061	4.13(9)	0.01364		$E1$	$<3.1\times10^{-4}$	1
		841.99	0	6_g^+	548	37.1(11)	0.00173		$E1$	$<1.7\times10^{-4}$	1
		1124.94	0	4_g^+	266	100(3)	0.00101		$E1$	$<1.9\times10^{-4}$	

Table 2 continued

E_i (keV)	J_i^π	E_γ (keV)	K_f	J_f^π	E_f (keV)	I_γ (rel.)	α_T	τ (fs)	$\pi\ell$	B($E1$) or B($E2$)	Notes
$K^\pi = 0_1^-$											
1275.73	1^-	1195.11	0	2_g^+	81	100(2)	9.23×10^{-4}	120(10)	$E1$	$9.2^{+1.3}_{-1.1} \times 10^{-4}$	
		1275.81	0	0_g^+	0	73.4(19)	8.61×10^{-4}		$E1$	$5.6^{+0.8}_{-0.7} \times 10^{-4}$	2
1357.86	3^-	1092.26	0	4_g^+	266	72(5)	0.00106	100(20)	$E1$	$1.1^{+0.4}_{-0.3} \times 10^{-3}$	3
		1277.27	0	2_g^+	81	100.0(19)	8.60×10^{-4}		$E1$	$9.2^{+3.0}_{-2.0} \times 10^{-4}$	
1518.39	5^-	160.49	0_1	3^-	1358	0.62(4)	0.499	270^{+80}_{-50}	$E2$	(See [b])	1
		457.49	2	4_γ^+	1061	0.15(4)	0.00628		$E1$	$1.3^{+0.8}_{-0.6} \times 10^{-5}$	1
		970.01	0	6_g^+	548	42(1)	0.00132		$E1$	$3.9^{+1.1}_{-1.0} \times 10^{-4}$	
		1252.74	0	4_g^+	266	100(2)	8.76×10^{-4}		$E1$	$4.3^{+1.2}_{-1.1} \times 10^{-4}$	
$K^\pi = 5_1^-$											
1485.71	5^-	95.16	2_1	5^-	1391	2.0(2)	3.0(3)	$<2910^\dagger$	$M1/E2$	(See [c])	1
		161.21	2	6_γ^+	1324	0.29(2)	0.0860		$E1$	$>4.5\times10^{-5}$	1
		188.66	2_1	4^-	1297	3.8(5)	0.350(14)		0.89(19)	>150	1
		275.58	2_1	3^-	1210	3.05(8)	0.0839		$E2$	>62	1
		302.91	2	5_γ^+	1183	1.26(3)	0.01679		$E1$	$>3.1\times10^{-5}$	1
		424.68	2	4_γ^+	1061	1.51(8)	0.00745		$E1$	$>1.3\times10^{-5}$	1
		937.23	0	6_g^+	548	35(2)	0.00141		$E1$	$>2.8\times10^{-5}$	
		1220.16	0	4_g^+	266	100(3)	9.01×10^{-4}		$E1$	$>3.7\times10^{-5}$	
$K^\pi = 3_1^-$											
1570.76	3^-	212.98	0_1	3^-	1358	59(1)	0.269(6)	–	0.47(7)	–	4
		295.23	0_1	1^-	1276	100(2)	0.0678		$E2$	–	
		360.82	2_1	3^-	1210	2.5(1)	0.065(5)		<0.64	–	1
		422.69	2_1	2^-	1148	3.5(4)	0.0238		$E2$	–	1
		682.77	2	2_γ^+	888	0.6(3)	0.00263		$E1$	–	1
1669.13	4^-	98.18	3_1	3^-	1571	0.17(6)	2.71(20)	440^{+450}_{-210}	$M1/E2$	(See [d])	1
		150.65	0_1	5^-	1518	15.3(4)	0.689(12)		0.92(9)	(See [e])	1
		278.57	2_1	5^-	1391	10.4(2)	0.134(5)		<0.39	<330	1
		311.27	0_1	3^-	1358	100(5)	0.1024		$M1$	–	
		372.07	2_1	4^-	1297	4.6(1)	0.061(3)		<0.48	<49	1
		459.00	2_1	3^-	1210	8.8(11)	0.0370		$M1$	–	1
		486.32	2	5_γ^+	1183	1.7(3)	0.00547		$E1$	$5.9^{+8.6}_{-3.7} \times 10^{-5}$	1
		520.89	2_1	2^-	1148	0.61(11)	0.01363		$E2$	$3.0^{+4.4}_{-1.9}$	1
		1403.25	0	4_g^+	266	23(8)	8.13×10^{-4}		$E1$	$3.3^{+6.0}_{-2.3} \times 10^{-5}$	1
$K^\pi = 1_1^-$											
1637.19	1^-	279.27	0_1	3^-	1358	1.2(3)	0.0805	–	$E2$	–	5
		361.42	0_1	1^-	1276	6.4(8)	0.053(16)		$M1/E2$	–	
		427.11	2_1	3^-	1210	14.7(8)	0.0231		$E2$	–	
		488.96	2_1	2^-	1148	15.4(12)	0.0238(77)		$M1/E2$	–	
		1556.50	0	2_g^+	81	100(14)	8.12×10^{-4}		$E1$	–	
		1637.32	0	0_g^+	0	24(2)	–		$E1$	–	

Table 2 continued

E_i (keV)	J_i^π	E_γ (keV)	K_f	J_f^π	E_f (keV)	I_γ (rel.)	α_T	τ (fs)	$\pi\ell$	B($E1$) or B($E2$)	Notes
1691.38	2^-	394.33	2_1	4^-	1297	12.1(6)	0.0289	–	$E2$	–	1
		415.57	0_1	1^-	1276	56(4)	0.036(12)		$M1/E2$	–	2
		728.50	2	3^+_γ	963	98(1)	0.00231		$E1$	–	
1739.01	3^-	168.09	3_1	3^-	1571	2.5(3)	0.528(23)	>740	<0.73	<520	1
		348.49	2_1	5^-	1391	5.1(13)	0.0412		$E2$	<89	1
		381.07	0_1	3^-	1358	4.4(3)	0.051(7)		0.7(4)	<23	1
		441.99	2_1	4^-	1297	5.0(3)	0.034(5)		0.7(4)	<12	1
		463.22	0_1	1^-	1276	13(1)	0.0185		$E2$	<48	1
		529.06	2_1	3^-	1210	100(2)	0.0257		1.4(2)	<130	
		590.74	2_1	2^-	1148	37(2)	0.0147(48)		$1.2^{+0.5}_{-0.3}$	<29	
		678.12	2	4^+_γ	1061	63(2)	0.00267		$E1$	$<3.2\times10^{-4}$	
		1473.36	0	4^+_g	266	66(1)	8.07×10^{-4}		$E1$	$<3.2\times10^{-5}$	
$K^\pi = 4^-_1$											
1862.96	4^-	228.26	4_1	5^+	1634	10.4(2)	0.0345	1716	$E1$	$9.0^{+1.4}_{-1.1}\times10^{-4}$	1 6
		327.13	4_1	4^+	1536	100(13)	0.01390		$E1$	$2.9^{+0.5}_{-0.4}\times10^{-3}$	
		377.02	5_1	5^-	1486	1.58(7)	0.047(15)		$M1/E2$	10^{+2}_{-1}	1
		652.58	2_1	3^-	1210	21.0(6)	0.00782		$E2$	$8.7^{+1.4}_{-1.1}$	1
		714.44	2_1	2^-	1148	50(7)	0.00633		$E2$	13^{+4}_{-3}	1
$K^\pi = 2^-_2$											
1863.84	2^-	588.8	0_1	1^-	1276	10(4)	–	420^{+120}_{-80}	$M1/E2$	25^{+22}_{-14}	1
		652.1	2_1	3^-	1210	15(3)	–		$M1/E2$	23^{+14}_{-10}	1
		900.91	2	3^+_γ	963	34(1)	–		$E1$	$1.8^{+0.7}_{-0.5}\times10^{-4}$	
		975.65	2	2^+_γ	888	100(2)	–		$E1$	$4.1^{+1.5}_{-1.2}\times10^{-4}$	
		1782.8	0	2^+_g	80	48(5)	–		$E1$	$3.2^{+1.5}_{-1.1}\times10^{-5}$	1
1910.48	3^-	552.49	0_1	3^-	1358	1.0(1)	0.0174(57)	550^{+260}_{-180}	$M1/E2$	$2.1^{+1.4}_{-0.8}$	1
		849.44	2	4^+_γ	1061	80(2)	0.00170		$E1$	$3.0^{+1.7}_{-1.0}\times10^{-4}$	1
		947.51	2	3^+_γ	963	100(2)	0.00138		$E1$	$2.7^{+1.5}_{-0.9}\times10^{-4}$	
		1022.32	2	2^+_γ	888	81(2)	0.00120		$E1$	$1.7^{+1.0}_{-0.6}\times10^{-4}$	
1973.09	4^-	678.05	2_1	3^-	1210	82(8)	–	780^{+280}_{-210}	$M1/E2$	53^{+31}_{-20}	1
		912.09	2	4^+_γ	1061	33(2)	–		$E1$	$8.5^{+4.6}_{-2.9}\times10^{-5}$	
		1010.19	2	3^+_γ	963	100(2)	–		$E1$	$1.9^{+0.9}_{-0.6}\times10^{-4}$	
$K^\pi = unk$											
2520.4	1^-	2440	0	2^+_g	81	100	0.00114	$11(1)^\dagger$	$E1$	$1.1^{+0.2}_{-0.1}\times10^{-3}$	7
		2520	0	0^+_g	0	84(6)	0.00118		$E1$	$8.5^{+1.9}_{-1.5}\times10^{-4}$	

Table 2 continued

E_i (keV)	J_i^π	E_γ (keV)	K_f	J_f^π	E_f (keV)	I_γ (rel.)	α_T	τ (fs)	$\pi\ell$	B($E1$) or B($E2$)	Notes
$K^\pi = unk$											
2929.4	1^-	2849	0	2_g^+	81	56(8)	0.00132	29(3)[†]	$E1$	$1.8^{+0.6}_{-0.5} \times 10^{-4}$	[7]
		2929	0	0_g^+	0	100	0.00135		$E1$	$2.9^{+0.5}_{-0.4} \times 10^{-4}$	

[1] This γ ray was not observed in this work, therefore the energy and intensity were adopted from Ref. [24].
[2] As this is a multiplet in our work, the energy and intensity of the γ ray was adopted from Ref. [24].
[3] Both γ rays from this level were observed in this work, but the one with the stronger intensity was a multiplet. Therefore, all information for this level was adopted from Ref. [24].
[4] This γ ray was observed in this work, but a mixing ratio was not measured. Therefore, all information (energy, intensity, and mixing ratio) was adopted from Ref. [24].
[5] Three γ rays from this level were observed in this work, but one of them was a multiplet and the intensities were only available as limits. Therefore, all information for this level was adopted from Ref. [24].
[6] The lifetime of this level was measured using the GRID method by Ref. [3], which reports lifetimes as a range. We adopt the $\tau = 0.6\tau_{max}$ convention used in the publication, following the approach originally introduced by Ref. [37].
[7] This level was not observed in our work. All information was adopted from Ref. [24] and used here for completion.
[a] A mixing ratio is not listed and there are no additional notes about this γ ray in Ref. [24]. However, a calculation of the B($E2$) value (assuming pure $E2$) using all available information results in $7.1^{+3.4}_{-4.0} \times 10^3$ W.u. Considering the measured lifetime and the RUL (1000 W.u.), the mixing ratio would be $\delta < 0.4$.
[b] This γ ray can only be pure $E2$ and there are no additional notes about it in Ref. [24]. However, a calculation of the B($E2$) value using all available information results in $2.3^{+0.8}_{-0.7} \times 10^3$ W.u., calling this γ ray into question.
[c] A mixing ratio is not listed and there are no additional notes about this γ ray in Ref. [24]. However, a calculation of the B($E2$) value (assuming pure $E2$) using all available information results in $>7.6\times10^3$ W.u. Considering the measured lifetime and the RUL, the mixing ratio would be $\delta < 0.4$.
[d] A mixing ratio is not listed and there are no additional notes about this γ ray in Ref. [24]. However, a calculation of the B($E2$) value (assuming pure $E2$) using all available information results in $3.5^{+6.5}_{-2.5} \times 10^3$ W.u. Considering the measured lifetime and the RUL, the mixing ratio would be $\delta < 0.6$.
[e] There are no additional notes about this γ ray in Ref. [24]. However, a calculation of the B($E2$) value using all available information results in $1.7^{+2.3}_{-1.0} \times 10^4$ W.u., calling this γ ray into question.

1^-, 2^-, 3^- in the low-lying spectra of well-deformed nuclei. The ordering of the negative parity bands in ^{162}Dy is difficult to predict apriori with modern models [2]. We observe the following bandheads from lowest to highest in the excitation spectrum of ^{162}Dy, $K^\pi=2_1^-$, $K^\pi=0_1^-$, $K^\pi=3_1^-$, $K^\pi=1_1^-$, and $K^\pi=2_2^-$ at 1148.4, 1275.5, 1570.9, 1637.2, and 1863.8 keV, respectively.

3.1.1 $K^\pi=2_1^-$ Band at 1148.4 keV

We are immediately presented with some of the limitations of DSAM in our measurement of the lifetime of the bandhead of the $K^\pi=2^-$ at 1148.4 keV. Lifetimes of the 3^-, 4^-, and 5^- members of this band have been measured in this work. γ rays can be heavily attenuated by the scattering target; while we correct for this γ absorption in the peak area, lifetimes from the Doppler shift of γ rays with energies below 500 keV are difficult to extract. Normally, DSAM measurements are reported at the lowest possible bombarding neutron energy, but due to this attenuation of low-energy γ rays, a more precise measurement of the lifetimes in this band is taken from the 2.2 MeV bombarding neutron data set. The vast majority of observed transitions displayed negative (or consistent with zero within 1σ uncertainty) F(τ) values.

Each state is strongly connected within the band and with collective transitions to the γ-vibrational states. This highly-favored trend of γ rays to the $K^\pi=2_\gamma^+$ band is difficult to ignore in the face of large B($E1$) values of 10^{-5} in comparison with 10^{-9} to the ground state. B($E1$) values from the 3^- member to the $K^\pi=2_\gamma^+$ band members are one order of magnitude higher than those to the ground state. The 4^- state of the same band shows three orders of magnitude preference to the $K^\pi=2_\gamma^+$ band over the ground state. The B($E1$) values are essentially the hindrance factors [27] for this set of $\Delta K = 0$ transitions to the $K^\pi=2_\gamma^+$. From each level of this band, the preferential decay is to the γ band and the B($E1$) values are orders of magnitude higher than those of the $\Delta K = 2$ transitions to the ground state. Pascu [15] stresses the importance of this preferential $K^\pi = 2^- \rightarrow K^\pi = 2^+$ decay in nearby nuclei via the measurement of direct $E3$ radiation as a potential octupole-quadrupole coupling; however, this decay pattern could be a product of K-forbiddenness, as any decays to the ground state involve ΔK=2 versus the ΔK=0 transitions to the γ band. We also mirror these same concerns on the continued study of interband decays in the rare-earth region to fully understand this band; B($E3 : 5^- \rightarrow 2_\gamma^+$) strengths would be remarkably useful in this aspect. This study of ^{162}Dy offers some distinct challenges in terms of the detection of radiation for low-lying excitations; for example,

Table 3 Comparison of $E1$ and $E2$ transition probabilities from the various K^π bands with the Alaga rules. Uncertainties were obtained by using the upper and lower bound values of each transition probability from Table 2 to obtain the highest and lowest possible ratios and finding the difference between them and the nominal value. The $K^\pi=0_1^-$ and the $K^\pi=1_3^-$ bands are collective excitations built on the ground state of ^{162}Dy. The $K^\pi=2_1^-$ and the $K^\pi=2_2^-$ bands are excitations built on the $K^\pi=2_\gamma^+$ band with excellent agreement with Alaga rules. The $K^\pi=1_1^-$ band has enhanced B($E2$) transition probabilities to both the $K^\pi=2_1^-$ and the $K^\pi=0_1^-$ bands, but the Alaga ratios show that it is not an excitation built on either band. The ground state band members are noted using "g"

	$\frac{J\to J'_f}{J\to J''_f}$	$(n,n'\gamma)$	Alaga	Notes
$K_i^\pi=2_1^-$:	$\frac{3^-\to 3^+_\gamma}{3^-\to 2^+_\gamma}$	$1.5^{+4.9}_{-1.2}$	1.4	
	$\frac{4^-\to 4^+_\gamma}{4^-\to 3^+_\gamma}$	$0.5^{+1.1}_{-0.4}$	0.6	
$K_i^\pi=0_1^-$:	$\frac{1^-\to 2^+_g}{1^-\to 0^+_g}$	$1.6^{+0.5}_{-0.3}$	2.0	
	$\frac{3^-\to 4^+_g}{3^-\to 2^+_g}$	$1.2^{+0.7}_{-0.5}$	1.3	
	$\frac{5^-\to 6^+_g}{5^-\to 4^+_g}$	$0.9^{+0.7}_{-0.4}$	1.2	
$K_i^\pi=2_2^-$:	$\frac{2^-\to 3^+_\gamma}{2^-\to 2^+_\gamma}$	$0.4^{+0.5}_{-0.2}$	0.5	
	$\frac{3^-\to 4^+_\gamma}{3^-\to 3^+_\gamma}$	$1.1^{+1.5}_{-0.6}$	1.3	
	$\frac{3^-\to 3^+_\gamma}{3^-\to 2^+_\gamma}$	$1.6^{+2.2}_{-0.9}$	1.4	
	$\frac{4^-\to 4^+_\gamma}{4^-\to 3^+_\gamma}$	$0.4^{+0.6}_{-0.2}$	0.6	
$K_i^\pi=3_1^-$ (to $K^\pi=2_1^-$):	$\frac{4^-\to 2^-_1}{4^-\to 4^-_1}$	>0.1	0.8	[1]
	$\frac{4^-\to 4^-_1}{4^-\to 5^-_1}$	0.1	1.2	[2]
$K_i^\pi=4_1^-$ (to $K^\pi=4_1^+$):	$\frac{4^-\to 5^+_1}{4^-\to 4^+_1}$	0.3(1)	0.3	
$K_i^\pi=4_1^-$ (to $K^\pi=2_1^-$):	$\frac{4^-\to 3^-_1}{4^-\to 2^-_1}$	0.7(3)	0.6	
$K_i^\pi=1_1^-$ (to $K^\pi=2_1^-$):	$\frac{3^-\to 5^-_1}{3^-\to 4^-_1}$	7.4	13.9	[2]
	$\frac{3^-\to 4^-_1}{3^-\to 3^-_1}$	0.09	0.14	[2]
	$\frac{3^-\to 3^-_1}{3^-\to 2^-_1}$	4.5	1.2	[2]
$K_i^\pi=1_1^-$ (to $K^\pi=0_1^-$):	$\frac{3^-\to 3^-_1}{3^-\to 1^-_1}$	0.5	0.15	[2]
$K_i^\pi=1_2^-$:	$\frac{1^-\to 2^+_g}{1^-\to 0^+_g}$	$1.3^{+0.6}_{-0.3}$	0.5	[3]
$K_i^\pi=1_3^-$:	$\frac{1^-\to 2^+_g}{1^-\to 0^+_g}$	$0.6^{+0.4}_{-0.2}$	0.5	[3]

[1] The B(E2: $4^-\to 4^-_1$) used for this ratio is an upper limit. We have expressed this ratio as a lower limit

[2] Both transition probabilities used for this ratio are upper limits. We report a ratio obtained from taking the nominal value of each transition probability

[3] The K value of this state is unknown. However, for the purpose of comparing with the Alaga rules, we have assumed this state to be $K_i^\pi=1^-$

measurement of the interband $2^-\to 3^+_\gamma$ transition lies at 185 keV, placing it directly in conflict with our most strongly populated $4^+_g\to 2^+_g$ transition. This experimental challenge is beyond the scope of the γ-ray-singles-based experiments performed in this work at UKAL, and would require coincidence measurements to observe those γ rays.

3.1.2 $K^\pi=0_1^-$ Band at 1275.7 keV

We have measured lifetimes for the 1^-, 3^-, and 5^- members of the $K^\pi=0_1^-$ band, currently assigned as the single octupole vibration in ^{162}Dy from literature B($E3: 3^-\to 0^+_g$) measurements ranging from $9.6-32.7$ W.u. [33,34].

As noted in Table 1, our level lifetime of 120(10) fs for the 1^- bandhead (shown in Fig. 1) differs from the ENSDF value of 29(6) fs, which was calculated from the direct B($E1$)↑

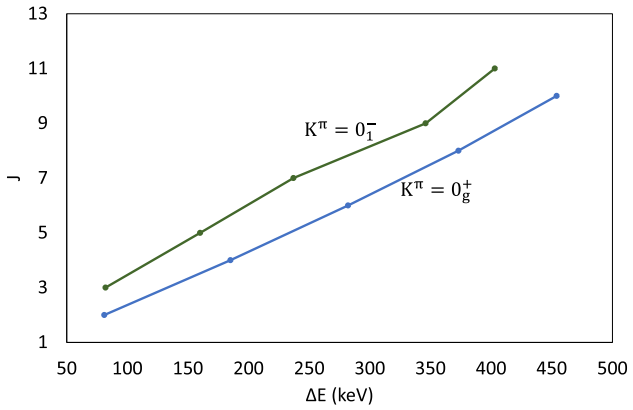

Fig. 2 Dynamic moments of inertia for the ground state and $K^\pi=0_1^-$ bands

measurement in Ref. [35]. The ENSDF evaluator calls this lifetime into question because the γ branches of $E1$ radiation depopulating the state differ drastically from the adopted values. We are confident in our lifetime determinations from the well-defined Doppler energy shifts of the two γ rays from this 1275.7 keV level and are in agreement with a more recent measurement from Ref. [3].

The transition probabilities from these states evince enhanced $E1$ decays to the ground state (Table 2) and exhibit agreement with the Alaga predictions (Table 3). Although these B($E1$)s are smaller overall than those from other confirmed single-phonon octupole vibrations in the region (^{168}Er [36]), the transition probabilities are well above the threshold for what is generally considered collective in the mass region ($\sim 10^{-5}$mW.u. strengths). Furthermore, our measured B(E1:$1^-_{K^\pi=0^-} \rightarrow 0^+_g$) of 0.56 mW.u. (0.001 e^2fm^2) compares reasonably with the systematic behavior of $E1$ strengths for the bandheads of $K^\pi=0^-$ bands in deformed rare-earth nuclei (B($E1$)$\sim$0.003$-$0.005 e^2fm^2) [37].

3.1.3 $K^\pi=3_1^-$ band at 1570.9 keV

The lifetime of the bandhead was not measured in this work and remains unknown, but we were able to extract a lifetime of 440^{+450}_{-210} fs for the 4^- state in this band at 1669.1 keV.

3.1.4 $K^\pi=1_1^-$ band at 1637.2 keV

The lifetimes of the 1_1^- bandhead and the 2^- member (1691.4 keV) are not known, but a lower limit (>740 fs) was determined for the 3^- state (1739.0 keV). From this band, the transition probabilities to the γ band are an order of magnitude larger than those to the ground state. There are, however, fairly collective B($E2$) values associated with the other negative parity states. The most favored in this case is to the $3^-_{K^\pi=3_1^-}$ state.

3.1.5 $K^\pi=2_2^-$ band at 1863.8 keV

There are three levels associated with the $K^\pi=2_2^-$ band including the 1863.8 keV bandhead, a 3^- at 1910.5 keV, and a 4^- at 1973.0 keV. This work measured lifetimes of 420^{+120}_{-80} fs, 550^{+260}_{-180} fs, and 780^{+280}_{-210} fs for the 2^-, 3^-, and 4^- members of the band, respectively. The B($E1$) values from the 3^- state show enhanced probabilities to the γ band.

4 Discussion

This study reports on the measured lifetimes of several negative and unknown parity states. The transition probabilities extracted from the lifetimes show interesting connections between several excited bands.

For the negative parity states, a significant step is the separation of the collective excitations built on the ground state from those that highlight components of the wave functions. Level lifetimes are used to characterize these negative parity states in terms of collective excitations, or the coupling of quadrupole and octupole modes, vs. single or double quasiparticle excitations, or something completely different. Furthermore, we can compare the B($E2$) and B($E1$) values with the Alaga rules to determine which states can be considered oscillations on other bands or the ground state.

The general trend is that the lowest $K^\pi=2_1^-$ band is strongly connected to the $K^\pi=2_\gamma^+$ band with B($E1$) values ranging from 1 to several mW.u. while those to the ground state band are an order of magnitude weaker. Transitions from the $K^\pi=2_1^-$ band were compared with the Alaga rules and show agreement, indicating that this band might be built on the $K^\pi=2_\gamma^+$ band (shown in Table 3). The $K^\pi=2_2^-$ band also shows enhanced $E1$ values to the γ band and shows good agreement with the Alaga rules, indicating it as another potential band built on the $K^\pi=2_\gamma^+$ band.

The $K^\pi=0_1^-$ band displays connections to the ground state band, ten times larger than transitions to the $K^\pi=2_\gamma^+$. When compared with the Alaga rules (Table 3), the transitions show good agreement, indicating that this band is possibly an excitation built on the ground state. This band has many more levels of unknown lifetimes, allowing for a comparison of its dynamic moment of inertia with that of the ground state band. Figure 2 shows that the dynamic moments of inertia of these two bands are nearly identical, further strengthening the possibility of this band being the 0^- component of an octupole oscillation on the deformed ground state.

The 5_1^- state at 1485.7 keV is connected to the 3^-, 4^-, and 5^- members of the $K^\pi=2_1^-$ band with significantly enhanced $E2$ transition probabilities. While this state appears to be a clear excitation built on the $K^\pi=2_1^-$ band, this surprising result is not yet understood and also involves a $\Delta K = 3$

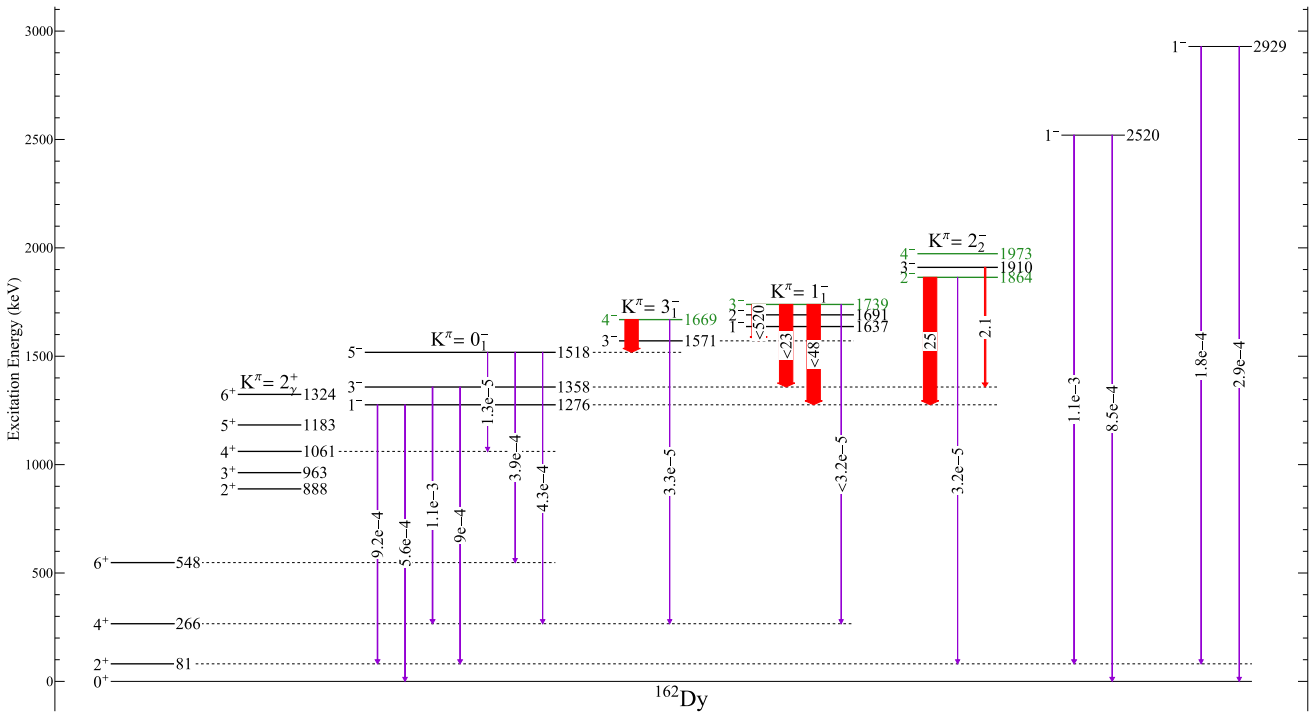

Fig. 3 Negative parity bands with strong transitions to the ground state band and/or $K^\pi=0_1^-$ bands. Levels with new lifetime measurements are drawn in green. All transitions are are expressed in Weisskopf units (W.u.). The B($E2$) values are in red while the B($E1$) values are in purple with proportional thicknesses

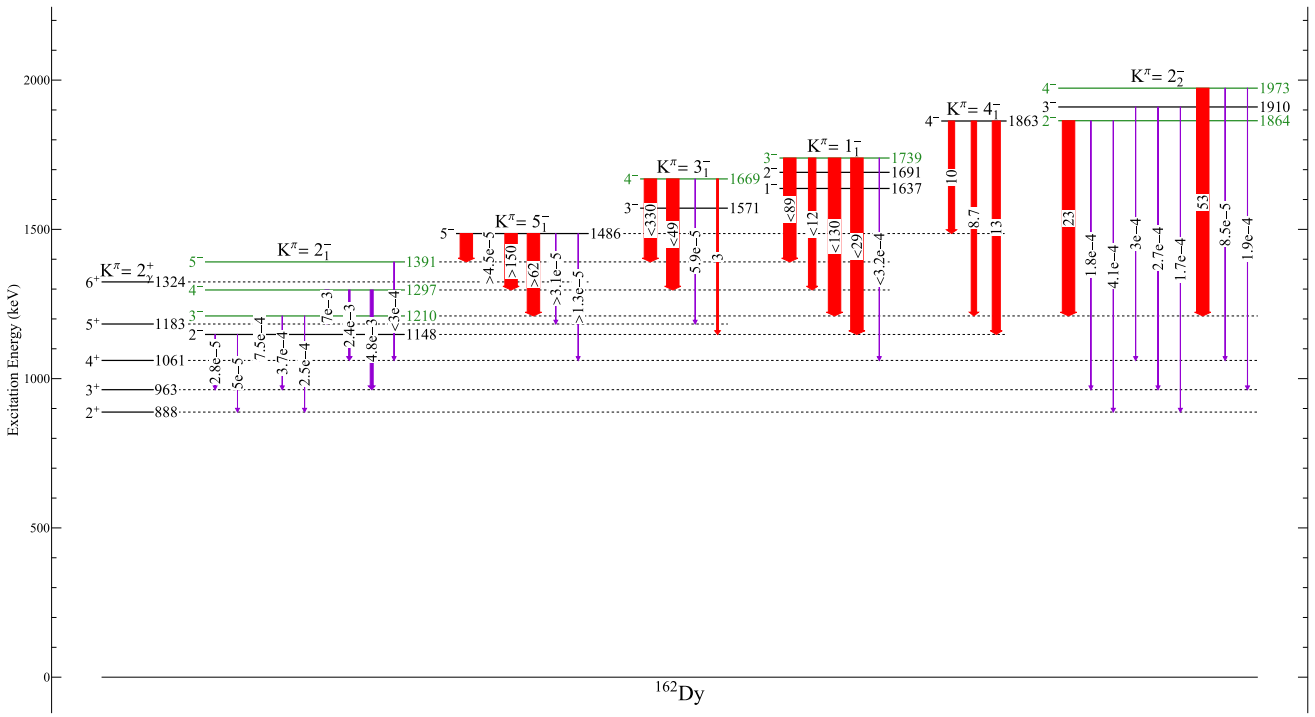

Fig. 4 Negative parity bands with strong transitions to the $K^\pi=2_\gamma^+$ and/or $K^\pi=2_1^-$ bands. Levels with new lifetime measurements are drawn in green. All transitions are expressed in Weisskopf units (W.u.). The B($E2$) values are in red while the B($E1$) values are in purple with proportional thicknesses

set of transitions. Self-consistent calculations of all even-even nuclei carried by the generator coordinate extension of the Hartree-Fock-Bogoliubov(HFB) mean field theory [4] in various theoretical frameworks have shown that in deformed nuclei, there are octupole correlations, but they tend to be weak. In addition, a similar calculation shows a two-quasi particle 5^- state at 1.2 MeV, almost 300 keV lower than the observed 5^- state at 1485.7 keV.

The $4^-_{K^\pi=3^-_1}$ state shows enhanced B($E2$) values to the $K^\pi=2^-_1$ band and a highly collective connection to the $K^\pi=0^-_1$ band that is two orders of magnitude larger. However, this also represents a $\Delta K = 3$ set of transitions, perhaps indicating an incorrect assignment of the state to this band. The transition probabilities to the $K^\pi=2^-_1$ band also show disagreement with the Alaga rules as shown in Table 3. This is probably also a two quasiparticle state.

The depopulating transition probabilities of the $K^\pi=1^-_1$ band favor the γ band with B($E1$) values that are an order of magnitude larger than those to the ground state. There are however, fairly large B($E2$) values to the other negative parity states. The most favored in this case is to the $3^-_{K^\pi=3^-_1}$ state. There are also large $E2$ transitions to several members of the $K^\pi=2^-_1$ and the $K^\pi=0^-_1$ bands. Of course, these B($E2$) values are upper limits since the lifetime measured was a lower limit. These transitions disagree with the Alaga rules for an excitation built on the $K^\pi=2^-_1$ band, indicating the relationship of quasi-particle components and not oscillations built on other bands.

There are additional level lifetime measurements shown in Table 2 with enhanced B($E1$) transition probabilities to the ground-state band without known K values with spins of 1^- at 2520.4 and 2929.4 keV. Both states show enhanced B($E1$) values to the ground state with those from the 1^-_2 (2520.4 keV) being an order of magnitude larger. In order to compare with the Alaga rules, we assumed that the unknown K values for the 1^- states are in fact $K^\pi=1^-$. The result is that the Alaga values disagree with considering the 1^-_2 state as an excitation built on the ground state. They do, however, agree for considering the 1^-_3 state (2929.4 keV) as an excitation built on the ground state. Of the three 1^- bands, we believe the 1^-_3 to be the 1^- component of an octupole oscillation on the deformed ground state.

Figure 3 shows the level scheme of negative parity bands with strong transitions to the ground state and $K^\pi = 0^-_1$ bands while Fig. 4 shows those with strong transitions to the $K^\pi=2^+_\gamma$ and $K^\pi = 2^-_1$ bands. Comparison of $E1$ and $E2$ transition probabilities from the various K^π bands with the Alaga rules are shown in Table 3. In this table, we can see potential vibrational excitations and states of other nature. The $K^\pi=0^-_1$ and the 1^-_3 bands are collective excitations built on the ground state of ^{162}Dy. The $K^\pi=2^-_1$ and the $K^\pi=2^-_2$ bands are excitations built on the $K^\pi=2^+_\gamma$ band with excellent agreement with Alaga rules. The $K^\pi=1^-_1$ band has enhanced B($E2$) transition probabilities to both the $K^\pi=2^-_1$ and the $K^\pi=0^-_1$ bands, but the Alaga ratios show that it is not an excitation built on either band. Figure 2 shows the dynamic moments of inertia for the $K^\pi=0^-_1$ and the ground state bands. The moments of inertia further indicate that this band is a potential octupole excitation built on the ground state band.

5 Conclusions

We measured the lifetimes of numerous negative parity levels in ^{162}Dy using the $(n, n'\gamma)$ reaction and the Doppler-shift attenuation method at the University of Kentucky. We report 14 new lifetimes measured across negative and unknown parity states. We presented our interpretations on the nature of several bands based on the extracted transition probabilities.

The $K^\pi=0^-_1$ and the 1^-_3 (assumed as $K^\pi = 1^-$) both show connections to the ground state band and agree in the ratio comparisons with the Alaga rules. We conclude that they are the fragmentation of octupole oscillations built on the ground state ^{162}Dy. While the 1^-_2 (assumed as $K^\pi = 1^-$) shows stronger connections to the ground state band than the 1^-_3, the Alaga values show that it cannot be considered as an excitation of the ground state. The $K^\pi=2^-_1$ and the $K^\pi=2^-_2$ bands are connected to the $K^\pi=2^+_\gamma$ band and show excellent agreement with the Alaga values. We believe these can be viewed as excitations built on the γ band, perhaps as octupole-quadrupole coupling to the γ band.

There are three bands we do not consider as excitations built on another band despite displaying strong connections. The $4^-_{K^\pi=3^-_1}$ state is connected to the $K^\pi=0^-_1$ and the $K^\pi=2^-_1$ bands with highly collective $E2$ transition probabilities, but the disagreement with the Alaga rules suggest otherwise, potentially as two quasiparticle states. The $K^\pi=1^-_1$ band exhibits similarly strong connections to the $K^\pi=0^-_1$ and the $K^\pi=2^-_1$ bands, but also disagrees with the Alaga rules. However, the enhanced B($E2$) values from this band clearly pick out some overlapping wave function components. Finally, the 5^- state shows enhanced B($E2$) values to the $K^\pi=2^-_1$ band, but its energy is approximately 300 keV higher than the expected energy of a two-quasi particle 5^- state.

The amount of lifetime information for the negative parity bands was greatly expanded by this work. No other nucleus in this region has such an extensive set of lifetime information for its negative parity bands. In the past, the absence of clear octupole-quadrupole coupling was attributed to the lack of lifetimes for negative parity states. This work partially addresses that need. The extracted transition probabilities connect the negative parity bands to each other and the γ band to reveal or identify common single or double quasi-particle excitation components of the bands. Hence,

we have the 0^- and the 1^- of the octuple quartet and two $K^\pi=2_1^-$ and $K^\pi=2_2^-$ bands that are excitations built on the $K^\pi=2_\gamma^+$. However, further experimental data is needed to be more conclusive about octupole oscillations in ^{162}Dy.

Acknowledgements We thank H. E. Baber for his contributions to accelerator maintenance and operation. This material is based upon work supported by the National Science Foundation (NSF) under grant numbers PHY-2411543, PHY-2310059, PHY-2209178, PHY-2022890, and in part by the U.S. Department of Energy's (DOE) National Nuclear Security Administration (NNSA), Grant DE-NA0004256). The enriched isotope used in this research was supplied by the United States Department of Energy Office of Science by the Isotope Program in the Office of Nuclear Physics.

Funding This work was funded by the National Science Foundation (NSF) under grant numbers PHY-2411543, PHY-2310059, PHY-2209178, PHY-2022890, and in part by the U.S. Department of Energy's (DOE) National Nuclear Security Administration (NNSA), Grant DE-NA0004256).

Data availability statement Data will be made available on reasonable request. [Authors' comment: The additional datasets reported here are available in the National Nuclear Database Center (NNDC). Data from this work will be made available from the corresponding author on reasonable request.]

Code availability statement Code/software will be made available on reasonable request. [Authors' comment: The code used during analysis of the data in this work is available from the corresponding author on reasonable request.]

References

1. A. Aprahamian, K. Lee, S.R. Lesher, R. Bijker, The nature of 0^+ excitations in deformed nuclei. Prog. Part. Nucl. Phys. **143**, 104173 (2025). https://doi.org/10.1016/j.ppnp.2025.104173
2. A. Aprahamian, X. Wu, S.R. Lesher, D.D. Warner, W. Gelletly, H.G. Börner, F. Hoyler, K. Schreckenback, R.F. Casten, Z.R. Shi, D. Kusnezov, M. Ibrahim, A.O. Macchiavelli, M.A. Brinkman, J.A. Becker, Complete spectroscopy of the ^{162}Dy nucleus. Nucl. Phys. A **764**, 42 (2006). https://doi.org/10.1016/j.nuclphysa.2005.09.020
3. A. Aprahamian, S.R. Lesher, C. Casarella, H.G. Börner, M. Jentschel, Lifetime measurements in ^{162}Dy. Phys. Rev. C **95**, 024329 (2017). https://doi.org/10.1103/PhysRevC.95.024329
4. L.M. Robledo, G.F. Bertsch, Global systematics of octupole excitations in even-even nuclei. Phys. Rev. C **84**, 054302 (2011). https://doi.org/10.1103/PhysRevC.84.054302
5. I. Ahmad, P.A. Bulter, Octupole shapes in nuclei. Annu. Rev. Nucl. Part. Sci. **43**, 71 (1993). https://doi.org/10.1146/annurev.ns.43.120193.000443
6. N.V. Zamfir, D. Kusnezov, Octupole correlations in U and Pu nuclei. Phys. Rev. C **67**, 014305 (2003). https://doi.org/10.1103/PhysRevC.67.014305
7. B. Bucher, S. Zhu, C.Y. Wu, R.V.F. Janssens, D. Cline, A.B. Hayes, M. Albers, A.D. Ayangeakaa, P.A. Butler, C.M. Butler, C.M. Campbell, M.P. Carpenter, C.J. Chiara, J.A. Clark, H.L. Crawford, M. Cromaz, H.M. David, C. Dickerson, E.T.G. Adn, J. Harker, C.R. Hoffman, B.P. Kay, F.G. Kondev, A. Korichi, T. Lauritsen, A.O. Macchiavelli, R.C. Pardo, A. Richard, M.A. Riley, G. Savard, M. Scheck, D. Seweryniak, M.K. Smith, R. Vondrasek, A. Wiens, Direct Evidence of Octupole Deformation in Neutron-Rich ^{144}Ba. Phys. Rev. Lett. **116**, 112503 (2016). https://doi.org/10.1103/PhysRevLett.116.112503
8. P.E. Garrett, W.D. Kulp, J.L. Wood, D. Bandyopadhyay, S. Choudry, D. Dashdorj, S.R. Lesher, M.T. McEllistrem, M. Mynk, J.N. Orce, S.W. Yates, New features of shape coexistence in ^{152}Sm. Phys. Rev. Lett. **103**, 062501 (2009). https://doi.org/10.1103/PhysRevLett.103.062501
9. J. Henderson, J. Heery, M. Rocchini, M. Siciliano, N. Sensharma, A.D. Ayangeakaa, R.V.F. Janssens, T.M. Kowalewski, P.D. Abhishek, E. Stevenson, B.A. Yüksel, T.R. Brown, L.M. Rodriguez, C.Y. Robledo, S. Wu, C. Kisyov, V. Müller-Gatermann, L. Bildstein, C.M. Canete, S. Campbell, M.P. Carmichael, W.N. Carpenter, P. Catford, C. Copp, M. Cousins, D.T. Devlin, P.E. Doherty, U. Garrett, L.P. Garg, K. Gaffney, D.J. Hadynska-Klek, S.F. Hartley, H. Hicks, S.R. Jayatissa, D. Johnson, F. Kalaydjieva, D. Kondev, T. Lascar, G. Lauritsen, N. Lotay, M. Marchini, S. Matejska-Minda, A. Nandi, C. Nannini, S. O'Shea, C.J. Pascu, A. Paxman, E.E. Perkoff, Z. Peters, A. Podolyák, R. Radich, B.J. Rathod, P.H. Reed, W. Regan, E. Reviol, R. Rubino, D. Russell, J.R. Seweryniak, G.L. Vanhoy, K. Wilson, S.W. Wrzosek-Lipska, I.Z. Yates, Deformation and collectivity in doubly magic ^{208}Pb. Phys. Rev. Lett. **134**, 062502 (2025). https://doi.org/10.1103/PhysRevLett.134.062502
10. R. Rodriguez-Guzman, L. Robledo, K. Nomura, N.C. Hernandez, Quadrupole-Octupole collectivity in the Xe, Ba, Ce, and Nd isotopic chains described with mean field and beyond approaches. J. Phys. G: Nucl. Part. Phys. **49**, 015101 (2022). https://doi.org/10.1088/1361-6471/ac3472
11. N. Minkov, P. Yotov, S. Drenska, W. Scheid, D. Bonatsos, D. Lenis, D. Petrellis, Nuclear collective motion with a coherent coupling interaction between quadrupole and octupole modes. Phys. Rev. C **73**, 044315 (2006). https://doi.org/10.1103/PhysRevC.73.044315
12. N. Minkov, S. Drenska, M. Strecker, W. Scheid, H. Lenske, Nonyrast nuclear spectra in a model of coherent quadrupole-octupole motion. Phys. Rev. C **85**, 034306 (2012). https://doi.org/10.1103/PhysRevC.85.034306
13. L.M. Robledo, G.F. Bertsch, Electromagnetic transition strengths in soft deformed nuclei. Phys. Rev. C **86**, 054306 (2012). https://doi.org/10.1103/PhysRevC.86.054306
14. U. Kneissl, A. Zilges, J. Margraf, I. Bauske, P. von Brentano, H. Friedrichs, R. Heil, R.D. Herzberg, H. Pitz, B. Schlitt, C. Wesselborg, First experimental evidence for two-phonon octupole-gamma-vibrational excitations in deformed nuclei. Phys. Rev. Lett. **71**, 2180 (1993)
15. S. Pascu, D. Buscurescu, G. Căta-Danil, V. Derya, M. Elvers, D. Filipescu, D.G. Ghită, T. Glodariu, A. Hennig, C. Mihai, N. Mărginean, R. Măginean, R. Mărginean, A. Negret, L. Netterdon, S.G. Pickerstone, T. Sava, M. Spieker, L. Stroe, N.V. Zamfir, A. Zilges, Detailed spectroscopy of quadrupole and octupole states in ^{168}Yb. Phys. Rev. C **91**, 034321 (2015). https://doi.org/10.1103/PhysRevC.91.034321

16. H. Maser, S. Lindenstruth, I. Bauske, O. Beck, P. von Brentano, T. Eckert, H. Friedrichs, R.D. Heil, R.D. Herzberg, A. Jung, U. Kneissl, J. Margraf, N. Pietralla, H.H. Pitz, C. Wesselborg, A. Zilges, Systematics of low-lying dipole excitations in the deformed even-even nuclei ^{164,166,168,170}Er. Phys. Rev. C **53**, 2749 (1996). https://doi.org/10.1103/PhysRevC.53.2749
17. A. Aprahamian, From ripples to tidal waves: low lying vibrational motion in nuclei. Nucl. Phys. A **731**, 291 (2004). https://doi.org/10.1016/j.nuclphysa.2003.11.040
18. X. Wu, A. Aprahamian, S.M. Fischer, W. Reviol, G. Liu, J.X. Saladin, Multiphonon vibrational states in deformed nuclei. Phys. Rev. C **49**, 1837 (1994). https://doi.org/10.1103/PhysRevC.49.1837
19. P.E. Garrett, N. Warr, S.W. Yates, Nuclear structure studies with the inelastic neutron scattering reaction and gamma-ray detection. J. Res. Natl. Inst. Stand. Technol. **105**, 141 (2000). https://doi.org/10.6028/jres.105.019
20. E. Sheldon, V. Rogers, Computation of total and differential cross section for compound nuclear reactions of the type (a, a), (a, a'), (a, b), (a, γ), (a, $\gamma-\gamma$), (a, bγ) and (a, b$\gamma-\gamma$): (IV) FORTRAN program 'CINDY'. Comput. Phys. Commun. **6**(3), 99–131 (1973). https://doi.org/10.1016/0010-4655(73)90049-0
21. T. Belgya, G. Molnár, S.W. Yates, Analysis of Doppler-shift attenuation measurements performed with accelerator-produced monoenergic neutrons. Nucl. Phys. A **607**, 43 (1996). https://doi.org/10.1016/0375-9474(96)00221-7
22. K.B. Winterbon, An analytic theory of doppler-shift attenuation. Nucl. Phys. A **246**, 293 (1975). https://doi.org/10.1016/0375-9474(75)90647-8
23. E.E. Peters, A. Chakraborty, B.P. Crider, B.H. Davis, M.K. Gnanamani, M.T. McEllistrem, F.M. Prados-Estévez, J.R. Vanhoy, S.W. Yates, Level lifetimes in the stable Zr nuclei: effects of chemical properties in Doppler-shift measurements. Phys. Rev. C **88**, 024317 (2013). https://doi.org/10.1103/PhysRevC.88.024317
24. N. Nica, Nuclear data sheets for A=162. Nucl. Data Sheets **195**, 1–367 (2024). https://doi.org/10.1016/j.nds.2024.04.001
25. K. Lee, A. Stratman, C. Casarella, A. Aprahamian, S. Lesher, TROPIC: a program for calculating reduced transition probabilities. Comput. Phys. Commun. **306**, 109383 (2025). https://doi.org/10.1016/j.cpc.2024.109383
26. P.A. Butler, W. Nazarewicz, Intrinsic reflection asymmetry in atomic nuclei. Rev. Mod. Phys. **68**, 349 (1996). https://doi.org/10.1103/RevModPhys.68.349
27. A. Aprahamian, E1 transitions in ^{168}Er. Phys. Rev. C **46**, 2093–2095 (1992). https://doi.org/10.1103/PhysRevC.46.2093
28. M. Spieker, S. Pascu, A. Zilgus, F. Iachello, Origin of low-lying enhanced e1 strength in rare-earth nuclei. Phys. Rev. Lett. **114**, 192504 (2015). https://doi.org/10.1103/PhysRevC.74.044312
29. N. Nica, Nuclear Data Sheets for A=160. Nucl. Data Sheets **176**, 1 (2021). https://doi.org/10.1016/j.nds.2021.08.001
30. C. Wesselborg, P. von Brentano, K. Zell, R. Heil, H. Pitz, U. Berg, U. Kneissl, S. Lindenstruth, U. Seemann, R. Stock, Photoexcitation of dipole modes in ^{162,162,164}Dy. Phys. Lett. B **207**(1), 22–26 (1988). https://doi.org/10.1016/0370-2693(88)90878-7
31. J. Margraf, T. Eckert, M. Rittner, I. Bauske, O. Beck, U. Kneissl, H. Maser, H.H. Pitz, A. Schiller, P. von Brentano, R. Fischer, R.D. Herzberg, N. Pietralla, A. Zilges, H. Friedrichs, Systematics of low-lying dipole strengths in odd and even Dy and Gd isotopes. Phys. Rev. C **52**, 2429–2443 (1995). https://doi.org/10.1103/PhysRevC.52.2429
32. O. Papst, V. Werner, J. Isaak, N. Pietralla, T. Beck, C. Bernards, M. Bhike, N. Cooper, B.P. Crider, U. Friman-Gayer, J. Kleemann, B. Krishichayan, F. Löher, E.E. Naqvi, F.M. Peters, R.S. Prados-Estévez, T.J. Ilieva, D. Ross, W. Savran, J.R.V. Tornow, Photo response of ^{164}Dy. Phys. Rev. C **102**, 034323 (2020). https://doi.org/10.1103/PhysRevC.102.034323
33. F.K. McGowan, W.T. Milner, Reduced M1, E1, E2 and E3 transition probabilities for transitions in $^{156-160}$Gd and $^{160-164}$Dy. Phys. Rev. C **23**, 1926 (1981). https://doi.org/10.1103/PhysRevC.23.1926
34. R.N. Oehlberg, L.L. Riedinger, A.E. Rainis, A.G. Schmidt, E.G. Funk, J.W. Mihelich, Coulomb excitation studies of ^{160}Dy, ^{162}Dy and ^{164}Dy. Nucl. Phys. A **219**, 543 (1974). https://doi.org/10.1016/0375-9474(74)90116-X
35. A. Zilges, P. von Brentano, H. Friedrichs, R.D. Heil, U. Kneissl, S. Lindenstruth, H.H. Pitz, C. Wesselborg, A survey of $\Delta K = 0$ dipole transitions from low lying $J = 1$ states in rare earth nuclei. Z. Phys. A **341**, 155 (1991). https://doi.org/10.1007/BF01303826
36. F.K. McGowan, W.T. Milner, R.L. Robinson, P.H. Stelson, Z.W. Grabowski, Coulomb excitation of vibrational-like states in 166 − 170Er. Nucl. Phys. A **297**, 51 (1978). https://doi.org/10.1016/0375-9474(78)90198-7
37. H.G. Börner, M. Jentschel, N.V. Zamfir, R.F. Casten, M. Krticka, W. Andrejtscheff, Ultrahigh resolution study of collective modes in ^{158}Gd. Phys. Rev. C **59**, 2432 (1999). https://doi.org/10.1103/PhysRevC.59.2432